The Assessment of Ride Quality of a Full Tractor and Trailer

Bor-Tsuen Wang, Associate Proessor
Po-I Hu, Graduate Student
Department of Mechanical Engineering
National Pingtung Polytechnic Institute
Pingtung, Taiwan 91207

Abstract

This paper presents an analytical model for the evaluation of ride comfort of tractor and trailer moving on an irregular road surface. The tractor and trailer are assumed to be rigid and subjected to the vertical and pitch motion only. The suspension systems and tires are considered to be linear viscouslly-damped spring elements. The vehicle is assumed to be symmetric along the moving direction. The wheel axle is modeled as an unsprung mass unit. A total number of 9 degree-of-freedom tractor and trailer ride model is developed and assumed to have a displacement input of stationary ergodic Gaussian random road profile. The frequency response functions of the system are first derived so as to determine the power spectral density functions of the system response. A conventional tractor and trailer is then used to simulate the vehicle response, and so forth the ride quality can be studied. The ride comfort of the driver seat is evaluated in comparison to the ISO 2631. The suspension travel, road holding, dynamic tire road and the acceleration distributions of the tractor and trailer which can affect the ride quality of parts and cargo are also studied. The effect of the vehicle speed, pay-load and road roughness on ride quality are systematically evaluated.
keywords: tractor and trailer, ride comfort, irregular road surface, vehicle model

I. Introduction

As the need of fast transportation, different kinds of tractors and trailers are frequently demanded. The ride quality of such a vehicle is a great deal of concern. The ride comfort of the driver is known greatly affecting the fatigue and the handling performance of the driver. The vibration amplitude of the cargo and the performance of the vehicle parts, such as the engine mounting, suspensions, tires and the wheel axles, are factors that will also affect the ride quality of the vehicles. The road condition plays an important role on the influence of ride quality; however, the road condition can not be sufficiently controlled. The proper design of vehicle components becomes the exclusive way to improve the ride quality.

The ride quality is generally evaluated by the ride comfort of the driver in comparison to comfort criteria. Various criteria have been developed to assess the ride comfort of the driver as well as the cargo. The ISO 2631 [1] provides a vibration level for defining human tolerance to whole-body vibration. The averaged absorbed power [2,3] associated with vertical and horizontal ride vibrations transmitted to the driver can be a measure of ride quality at driver's location. The comfort index [4,5] rated between 1 and 5 can be adopted to evaluate the ride comfort of passenger or cargo.

The development of ride model is the primary task to study the ride quality of a vehicle. A quarter car model is the simple one and frequently used for the assessment of ride quality [6-8]. The suspension and tire can be modeled as a linear spring damper element for its convenience and simplicity. The seat cushion can also be included in the dynamic model. To further and realistically represent the vehicle dynamics, either a half or full vehicle model can be developed based on the need of analysis objectives [9,10]. The half vehicle model can usually provide the vertical and longitudinal responses, while the full model can additionally study the roll and lateral responses. The flexibility of vehicle body is known critical to the response. The beaming effect is sometimes included in the ride model [11-12].

Some nonlinear effects for suspensions and tires can also be considered [13,14]. Through the linearization technique [15-17], the system response can be usually obtained. Depending on different types of road surface conditions, either protruding surface, periodically uneven road or random road profile, different analysis procedures can be adopted [18]. The frequency domain analysis [19,20] is generally adopted for the random excitation, while the time domain analysis [21] can be used for specific types for road inputs.

This paper concerns the development of a half model of full tractor and trailer for ride quality analysis. An irregular random road profile is considered as the road input; therefore. the frequency domain analysis is adopted in the paper. The ride quality parameters, including the ride comfort of the driver, accelerations at the different tractor and trailer locations, suspension travel, road holding and dynamic tire road are studied. The effects of vehicle speeds, pay-loads and road conditions are also considered. The developed analytical riding model can also be utilized for the optimum design of the system parameters.

II. Full Tractor and Trailer Riding Model

The 9 DOF vehicle riding model is shown in Fig. 1 z_1, z_2, z_3 and z_4 are the response coordinates of the unsprung masses m_1, m_2, m_3, m_4; z_5 and θ_1 are the vertical and pitch response coordinates of the tractor, θ_2 and θ_3 are the pitch response of draw bar and trailer respectively. The following assumptions are made:

1. The vehicle is moving at a constant forward speed over an uneven road.
2. The vehicle units (tractor, draw bar and trailer) are rigid.
3. The vehicle units are symmetric about forward direction.
4. The tractor and trailer can translate in the vertical and pitch directions only.
5. The unsprung mass (wheel axle weight) is assumed to

be connected between the suspension and the tire.

6. Tires are simulated as point contact models.
7. The tire and suspension are respectively assumed to be a linear-spring-damper.

The equations of motion of the full tractor trailer can be derived as follows:

$$[M]\{\ddot{y}\}+[C]\{\dot{y}\}+[K]\{y\}=[c']\{\dot{x}\}+[k']\{x\} \qquad (1)$$

where

$$\{y\}^T=\{z_1\ \ z_2\ \ z_3\ \ z_4\ \ z_5\ \ z_6\ \ \theta_1\ \ \theta_2\ \ \theta_3\}=\{y_1\ \ y_2\ \ y_3\ \ y_4\ \ y_5\ \ y_6\ \ y_7\ \ y_8\ \ y_9\} \qquad (2)$$

$$\{x\}^T=\{x_1\ \ x_2\ \ x_3\ \ x_4\} \qquad (3)$$

$\{y\}$, $\{\dot{y}\}$ and $\{\ddot{y}\}$ are the displacement, velocity and acceleration vectors of the output response coordinates respectively. $\{x\}$ and $\{\dot{x}\}$ are the displacement and velocity vectors of the input road profile respectively. $[M]$,$[C]$,$[K]$,$[C']$,$[K']$ are shown in Appendix A.

B. Definition Laden Conditions

In the paper, the cargo is assumed to be a particle and its locations are defined as l_{w_1} and l_{w_2} in front of the center gravity of tractor/trailer respectively. w_1 and w_2 are the loading capacities of the tractor and trailer, and R_{w_1} and R_{w_2} are the ratio of the loading conditions. So the parameters can be redefined as follows:

$$l_1'=l_1-((R_{w_1}*w_1)/(R_{w_1}*w_1+m_5))*l_{w_1} \qquad (4)$$

$$l_2'=l_2+((R_{w_1}*w_1)/(R_{w_1}*w_1+m_5))*l_{w_1} \qquad (5)$$

$$l_3'=l_3-((R_{w_2}*w_2)/(R_{w_2}*w_2+m_7))*l_{w_2} \qquad (6)$$

$$l_4'=l_4+((R_{w_2}*w_2)/(R_{w_2}*w_2+m_7))*l_{w_2} \qquad (7)$$

$$l_7'=l_7+((R_{w_1}*w_1)/(R_{w_1}*w_1+m_5))*l_{w_1} \qquad (8)$$

$$l_8'=l_8-((R_{w_2}*w_2)/(R_{w_2}*w_2+m_7))*l_{w_2} \qquad (9)$$

$$l_9'=l_9-((R_{w_1}*w_1)/(R_{w_1}*w_1+m_5))*l_{w_1} \qquad (10)$$

$$l_{11}'=l_{11}+((R_{w_2}*w_2)/(R_{w_2}*w_2+m_7))*l_{w_2} \qquad (11)$$

$$m_5'=m_5+R_{w_1}*w_1 \qquad (12)$$

$$I_5'=I_5+m_5*(((R_{w_1}*w_1)/(R_{w_1}*w_1+m_5))*l_{w_1})^2+(R_{w_1}*w_1)*$$
$$(l_{w_1}-((R_{w_1}*w_1)/(R_{w_1}*w_1+m_5))*l_{w_1}')^2 \qquad (13)$$

$$m_7'=m_7+R_{w_2}*w_2 \qquad (14)$$

$$I_7'=I_7+m_7*(((R_{w_2}*w_2)/(R_{w_2}*w_2+m_7))*l_{w_2})^2+(R_{w_2}*w_2)*$$
$$(l_{w_2}-((R_{w_2}*w_2)/(R_{w_2}*w_2+m_7))*l_{w_2})^2 \qquad (15)$$

The symbols with prime represents the parameters under loading conditions.

III. Road Model

A. Power Spectral Density Function of the Random Road Profiles

In order to investigate the vehicle riding characteristics, various forms of ground inputs have been developed. In this work, the ISO road roughness model (Class A-H) is adopted [22]. The power spectral density (PSD) function of the ground surface can be expressed as follows:

$$S_g(\Omega)=S_g(\Omega_0)\left(\frac{\Omega}{\Omega_0}\right)^{-N_1},\Omega\le\Omega_0 \qquad (16)$$

$$S_g(\Omega)=S_g(\Omega_0)\left(\frac{\Omega}{\Omega_0}\right)^{-N_2},\Omega>\Omega_0 \qquad (17)$$

where,

Ω_0: the reference spatial frequency, $1/2\pi$(cycles/m)

$S_g(\Omega_0)$: degree of roughness(cycles/m)

$N_1=2$

$N_2=1.5$

Ω: spatial frequency(cycles/m)

The values of $S_g(\Omega_0)$ [22] for different classes of road is listed in Table 1. It is more convenient to express the PSD function of ground profile as the function of temporal frequency in Hz for vehicle vibration analysis. The spatial frequency Ω in cycles/m can be transformed to the temporal frequency f in Hz as follows:

$$f=\Omega v \qquad (18)$$

where v is the vehicle speed in m/s. Therefore, the PSD function of ground profile can also be transformed and expressed in terms of the temporal frequency f as follow:

$$S_g(f)=S_g(\Omega)/v=S_g\left(\frac{f}{v}\right) \qquad (19)$$

B. Determination of Input Power Spectral Density Matrix $[S_{xx}(f)]$

The correlation function between $x_i(t)$ and $x_j(t)$ can be defined as follows [23]

$$R_{x_ix_j}(\tau)=\mathrm{E}[x_i(t)x_j(t+\tau)] \qquad (20)$$

The spectral density function can then be defined as the Fourier transform of the correlation function

$$S_{x_ix_j}=\int_{-\infty}^{\infty}R_{x_ix_j}(\tau)e^{-j2\pi f\tau}d\tau \qquad (21)$$

The ground profile inputs, $x_1(t)$, $x_2(t)$, $x_3(t)$ and $x_4(t)$, hold on the relationships for vehicle running at a constant speed v

$$x_1(t)=x_2(t+t_{d1}) \qquad (22)$$

$$x_1(t)=x_3(t+t_{d2}) \qquad (23)$$

$$x_1(t)=x_4(t+t_{d3}) \qquad (24)$$

where

$$t_{d_1}=\frac{l_1+l_2}{v} \tag{25}$$

$$t_{d_2}=\frac{l_1+l_2+l_5+l_6+l_8-l_3}{v} \tag{26}$$

$$t_{d_3}=\frac{l_1+l_2+l_5+l_6+l_8+l_4}{v} \tag{27}$$

In which t_{d1} is the delaying time between the front wheel of the tractor and the rear wheels of the tractor; t_{d2} is the delaying time between the front wheel of the tractor and the front wheel of the trailer; and t_{d3} is the delaying time between the front wheel of the tractor and the rear wheel of the trailer.

Let $R_{x_i x_j}(\tau)=R_{ij}(\tau)$ and $S_{x_i x_j}(f)=S_{ij}(f)$ for simplicity. The correlation function between $x_1(t)$ and $x_2(t)$, $R_{12}(\tau)$, can be shown as follows:

$$R_{12}(\tau)=\mathrm{E}[x_1(\tau)x_2(t+\tau)]=\mathrm{E}[x_1(t)x_1(t-t_d+\tau)]=R_{11}(t-t_d) \tag{28}$$

The spectral density function $S_{12}(f)$ can be obtained from Eq.(21); therefore, the input spectral density matrix $[S_{xx}(f)]$ can be obtained as follows:

$$[S_{xx}(f)]=S_g(f)\begin{bmatrix} 1 & e^{-j2\pi f t_{d_1}} & e^{-j2\pi f t_{d_2}} & e^{-j2\pi f t_{d_3}} \\ e^{j2\pi f t_{d_1}} & 1 & e^{-j2\pi f(t_{d_2}-t_{d_1})} & e^{-j2\pi f(t_{d_3}-t_{d_1})} \\ e^{j2\pi f t_{d_2}} & e^{j2\pi f(t_{d_2}-t_{d_1})} & 1 & e^{-j2\pi f(t_{d_3}-t_{d_2})} \\ e^{j2\pi f t_{d_3}} & e^{j2\pi f(t_{d_3}-t_{d_1})} & e^{j2\pi f(t_{d_3}-t_{d_2})} & 1 \end{bmatrix} \tag{29}$$

It is noted that $S_g(f)$ is shown in Eq.(19).

IV. Determination of System Transfer Function Matrix $[H_{xy}(f)]$

The equations of motion shown in Eq. (1) can be taken Laplace transform and become

$$([M]s^2+[C]s+[K])\{Y(s)\}=([C']s+[K'])\{X(s)\} \tag{30}$$

Let

$$[G(s)]=[M]s^2+[C]s+[K] \tag{31}$$

and

$$[P(s)]=[C']s+[K'] \tag{32}$$

then

$$[G(s)]\{Y(s)\}=[P(s)]\{X(s)\} \tag{33}$$

$$\{Y(s)\}=[G(s)]^{-1}[P(s)][X(s)]=[H_{xy}(s)]^T\{X(s)\} \tag{34}$$

where

$$[G(s)]^{-1}[P(s)]=[H_{xy}(s)]^T \tag{35}$$

one can easily replace s by $j\omega$ $(=j2\pi f)$, such that

$$\{Y(f)\}=[H_{xy}(f)]^T\{X(f)\} \tag{36}$$

V. Frequency Domain Analysis

A. System Output PSD $[S_{yy}(f)]$, $[S_{xy}(f)]$

For a multiple-input and multiple-output model, the Fourier Transform of the input and output vectors can then be derived as:

$$\{X(f)\}=\begin{Bmatrix} X_1(f) \\ X_2(f) \\ \vdots \\ X_n(f) \end{Bmatrix},\qquad \{Y(f)\}=\begin{Bmatrix} Y_1(f) \\ Y_2(f) \\ \vdots \\ Y_n(f) \end{Bmatrix} \tag{37}$$

The input and output spectral density matrices can also be defined as follows [23] :

$$[S_{yy}(f)]=\lim_{T\to\infty}\frac{1}{T}E\left[\{Y(f)\}^*\{Y(f)\}^T\right] \tag{38}$$

$$[S_{xx}(f)]=\lim_{T\to\infty}\frac{1}{T}E\left[\{X(f)\}^*\{X(f)\}^T\right] \tag{39}$$

so can be the crossspectral density matrix between the input and output vectors

$$[S_{xy}(f)]=\lim_{T\to\infty}\frac{1}{T}E\left[\{X(f)\}^*\{Y(f)\}^T\right] \tag{40}$$

where E[ ] represents the expected value; superscripts * and T denote complex conjugate and matrix transpose operations respectively. In practice, only finite time records are used to obtain Fourier Transform pairs. The i-th row and j-th column component of spectral density matrix $[S_{yy}]$ can be shown as follows:

$$S_{y_i y_j}=\lim_{T\to\infty}\frac{1}{T}E\left[Y_i(f)^*Y_j(f)^T\right] \tag{41}$$

From the definition of spectral density matrices, one can obtain

$$[S_{yy}(f)]=[H_{xy}(f)]^{T*}[S_{xx}(f)][H_{xy}(f)] \tag{42}$$

The PSD matrix of output parameters can be determined from the system transfer function and the PSD matrix of input parameters. Similarly. One can get

$$[S_{xy}(f)]=[S_{xx}(f)][H_{xy}(f)] \tag{43}$$

It is noted that $[S_{xx}(f)]$ is the PSD matrix of the ground input defined in Eq.(29), and $[H_{xy}(f)]$ is the system transfer function as defined in Eq.(35)

B. Ride Quality Parameters

1. Driver seat acceleration

The spectral density function of the driver seat which response coordinate is y_6 can be obtained as follows:

$$S_{\ddot{y}_6\ddot{y}_6}=(2\pi f)^4 S_{y_6y_6} \tag{44}$$

where $S_{y_6y_6}$ is the 6[th] row and 6[th] column element of $[S_{yy}(f)]$ defined in Eq. (42)

2. Suspension travel

The suspension travels of the front and rear suspensions of the tractor/trailer can be obtained as follows:

$$\delta_1(t) = y_5(t) + l_1 y_7(t) - y_1(t) \tag{45}$$

$$\delta_2(t) = y_5 + l_2 y_7(t) - y_2(t) \tag{46}$$

$$\delta_3(t) = y_5 + l_2 y_7(t) + (l_5 + l_6) y_8(t) + (l_8 - l_3) y_9(t) - y_3 \tag{47}$$

$$\delta_4(t) = y_5 + l_2 y_7(t) + (l_5 + l_6) y_8(t) + (l_8 + l_3) y_9(t) - y_4 \tag{48}$$

The spectral density functions of the front and rear suspension travels of the tractor/trailer can then be derived.

$$S_{\delta_1\delta_1} = S_{y_5y_5} - l_1 S_{y_7y_5} - S_{y_1y_5} - l_1 S_{y_5y_7} + l_1^2 S_{y_7y_7} + l_1 S_{y_1y_7} - S_{y_5y_1} + l_1 S_{y_7y_1} + S_{y_1y_1} \tag{49}$$

$$S_{\delta_2\delta_2} = S_{y_5y_5} + l_2 S_{y_7y_5} - S_{y_2y_5} + l_2 S_{y_5y_7} + l_2^2 S_{y_7y_7} - l_2 S_{y_2y_7} - S_{y_5y_2} - l_2 S_{y_7y_2} + S_{y_2y_2} \tag{50}$$

$$\begin{aligned} S_{\delta_3\delta_3} = {} & S_{y_5y_5} + l_7 S_{y_7y_5} + (l_5+l_6) S_{y_8y_5} + (l_8-l_3) S_{y_9y_5} - S_{y_3y_5} + l_7 S_{y_5y_7} + l_7^2 S_{y_7y_7} + l_7(l_5+l_6) S_{y_8y_7} + l_7(l_8-l_3) S_{y_9y_7} \\ & - l_7 S_{y_3y_7} + (l_5+l_6) S_{y_5y_8} + l_7(l_5+l_6) S_{y_7y_8} + (l_5+l_6)^2 S_{y_8y_8} + (l_8-l_3)(l_5+l_6) S_{y_9y_8} - (l_5+l_6) S_{y_3y_8} \\ & + (l_8-l_3) S_{y_5y_9} + l_7(l_8-l_3) S_{y_7y_9} + (l_5+l_6)(l_8-l_3) S_{y_8y_9} + (l_8-l_3)^2 S_{y_9y_9} - (l_8-l_3) S_{y_3y_9} \\ & - S_{y_5y_3} - l_7 S_{y_7y_3} - (l_5+l_6) S_{y_8y_3} - (l_8-l_3) S_{y_9y_3} + S_{y_3y_3} \end{aligned} \tag{51}$$

$$\begin{aligned} S_{\delta_4\delta_4} = {} & S_{y_5y_5} + l_7 S_{y_7y_5} + (l_5+l_6) S_{y_8y_5} + (l_8+l_4) S_{y_9y_5} - S_{y_4y_5} + l_7 S_{y_5y_7} + l_7^2 S_{y_7y_7} + l_7(l_5+l_6) S_{y_8y_7} + l_7(l_8+l_4) S_{y_9y_7} - l_7 S_{y_4y_7} \\ & + (l_5+l_6) S_{y_5y_8} + l_7(l_5+l_6) S_{y_7y_8} + (l_5+l_6)^2 S_{y_8y_8} + (l_8+l_4)(l_5+l_6) S_{y_9y_8} - (l_5+l_6) S_{y_4y_8} \\ & + (l_8+l_4) S_{y_5y_9} + l_7(l_8+l_4) S_{y_7y_9} + (l_5+l_6)(l_8+l_4) S_{y_8y_9} + (l_8+l_4)^2 S_{y_9y_9} - (l_8+l_4) S_{y_4y_9} \\ & - S_{y_5y_4} - l_7 S_{y_7y_4} - (l_5+l_6) S_{y_8y_4} - (l_8+l_4) S_{y_9y_4} + S_{y_4y_4} \end{aligned} \tag{52}$$

3. Road holding

The road holdings of the front and rear tires of the tractor and trailer can be defined as follows:

$$h_1(t) = y_1(t) - x_1(t) \tag{53}$$

$$h_2(t) = y_2(t) - x_2(t) \tag{54}$$

$$h_3(t) = y_3(t) - x_3(t) \tag{55}$$

$$h_4(t) = y_4(t) - x_4(t) \tag{56}$$

when $h_i(t)$ are positive, the wheels and the road remain contact. The spectral density functions of the road holdings can be derived.

$$S_{h_1h_1} = S_{y_1y_1} - S_{y_1x_1} - S_{x_1y_1} + S_{x_1x_1} \tag{57}$$

$$S_{h_2h_2} = S_{y_2y_2} - S_{y_2x_2} - S_{x_2y_2} + S_{x_2x_2} \tag{58}$$

$$S_{h_3h_3} = S_{y_3y_3} - S_{y_3x_3} - S_{x_3y_3} + S_{x_3x_3} \tag{59}$$

$$S_{h_4h_4} = S_{y_4y_4} - S_{y_4x_4} - S_{x_4y_4} + S_{x_4x_4} \tag{60}$$

4. Dynamic tire load

The contact forces between tires and road surfaces can also be shown as follows:

$$f_1(t) = k_{t_1} x_1(t) + c_{t_1} \dot{x}_1(t) \tag{61}$$

$$f_2(t) = k_{t_2} x_2(t) + c_{t_2} \dot{x}_2(t) \tag{62}$$

$$f_3(t) = k_{t_3} x_3(t) + c_{t_3} \dot{x}_3(t) \tag{63}$$

$$f_4(t) = k_{t_4} x_4(t) + c_{t_4} \dot{x}_4(t) \tag{64}$$

The spectral density functions of contact forces between tires and road surfaces can be obtained as:

$$S_{f_1} = \left(k_{t_1} + (2\pi f)^2 c_{t_1}\right) S_{h_1h_1} \tag{65}$$

$$S_{f_2} = \left(k_{t_2} + (2\pi f)^2 c_{t_2}\right) S_{h_2h_2} \tag{66}$$

$$S_{f_3} = \left(k_{t_3} + (2\pi f)^2 c_{t_3}\right) S_{h_3h_3} \tag{67}$$

$$S_{f_4} = \left(k_{t_4} + (2\pi f)^2 c_{t_4}\right) S_{h_4h_4} \tag{68}$$

5. Tractor and trailer body acceleration

$\bar{z}_1 \sim \bar{z}_{12}$ are defined as the locations of tractor/trailer as shown in Fig. 2. $\bar{z}_1 \sim \bar{z}_6$ are the locations in the tractor, and $\bar{z}_7 \sim \bar{z}_{12}$ are the locations in the trailer. The $\bar{z}_i$ and its spectral density function can be derived as follows:

(1) For i = 1 to 3

$$\bar{z}_i = y_5 - l_{z_i} y_7$$

$$S_{z_iz_i} = S_{y_5y_5} - l_{z_i} S_{y_5y_7} - l_{z_i} S_{y_7y_5} + l_{z_i}^2 S_{y_7y_7} \tag{69}$$

(2) For i = 4 to 6

$$\bar{z}_i = y_5 + l_{z_i} y_7$$

$$S_{z_iz_i} = S_{y_5y_5} + l_{z_i} S_{y_5y_7} + l_{z_i} S_{y_7y_5} + l_{z_i}^2 S_{y_7y_7} \tag{70}$$

(3) For i = 7 to 12

$$\bar{z}_i = y_5 + l_7 y_7 + (l_5 + l_6) y_8 + l_{z_i} y_9$$

$$\begin{aligned} S_{z_iz_i} = {} & S_{y_5y_5} + l_7 S_{y_7y_5} + (l_5+l_6) S_{y_8y_5} + l_{z_i} S_{y_9y_5} + l_7 S_{y_5y_7} + l_7^2 S_{y_7y_7} + (l_5+l_6) S_{y_5y_8} \\ & + l_7 (l_5+l_6) S_{y_7y_8} + (l_5+l_6)^2 S_{y_8y_8} + l_{z_i} (l_5+l_6) S_{y_9y_8} + l_{z_i} S_{y_5y_9} + l_7 l_{z_i} S_{y_7y_9} \\ & + (l_5+l_6) l_7 S_{y_8y_7} + l_7 l_{z_i} S_{y_9y_7} + (l_5+l_6) l_{z_i} S_{y_8y_9} + l_{z_i}^2 S_{y_9y_9} \end{aligned} \tag{71}$$

C. RMS Acceleration in 1/3 Octave Band

The PSD function of the acceleration can be obtained from the PSD function of the displacement as follows:

$$S_{\ddot{y}\ddot{y}}(f) = (2\pi f)^4 S_{yy}(f) \tag{72}$$

where $S_{\ddot{y}\ddot{y}}(f)$ is PSD function of acceleration. The RMS (root mean square) acceleration at a given center frequency f_c in 1/3 octave band can be determined by:

$$\ddot{y}_{1/3-RMS} = \left[\int_{f_l}^{f_u} S_{\ddot{y}\ddot{y}}(f)\,df\right]^{\frac{1}{2}} \tag{73}$$

$$f_u = 2^{1/6} f_c$$

$$f_l = 2^{-1/6} f_c$$

where

$\ddot{y}_{1/3-RMS}$: RMS acceleration in 1/3 octave band

f_c: central frequency

f_u: upper band frequency

f_l: lower band frequency

The upper central frequency is $2^{1/3}$ times the lower. The RMS values of vertical accelerations at the driver's seat in 1/3 Octave Band can be computed and compared with the reduced comfort boundaries recommended by ISO 2631 [1] to evaluate the ride comfort. Fig.3 shows the limits of whole-body vibration for fatigue in vertical direction.

D. Standard Deviation of the System Parameters

The standard deviation of the system parameters acceleration can also be obtained for zero mean values as follows:

$$\sigma_z = \left[\int_{f_1}^{f_2} S_{zz}(f)df\right]^{\frac{1}{2}} \tag{74}$$

where Z is any of the system parameters; $S_{zz}(f)$ is the PSD function of Z, and σ_z denotes the standard deviation of Z

VII. Results and Discussion

A conventional full tractor and trailer, which parameters are listed in Appendix C, is adopted for the following analytical simulation. Firstly, the RMS acceleration of the driver seat in 1/3 octave band which are compared with the ISO 2631 ride comfort criteria [1]. The characteristics of the system parameters, including the suspension travels, road holdings and contact forces between the tires and the road surface, are also studied. Finally, the acceleration response over the tractor and trailer are presented and can be utilized to evaluate the ride quality of the cargo. Throughout the simulation analysis, different vehicle speeds, road surface conditions and laden conditions are considered. It is noted that the suspension parameters are not optimum in this paper.

A. Characteristics of Transfer Functions

Table 2 shows the natural frequencies of the system considering the half/half laden conditions, i.e. half-laden in the tractor and half-laden in the trailer. Four natural frequencies near 5 Hz which can be recognized as the unsprung mass natural frequencies. The others are then related to the sprung mass units, including the driver seat, draw bar, the tractor and the trailer.

The system transfer functions between the input and output coordinates can be derived as shown in Eq. (35). Fig. 4 shows the amplitudes of the system transfer functions for the half/half laden condition. Figs. 4(a)-4(d) represent the transfer functions between the tire/road contact points and the unsprung mass units (wheel axles). For H_{ii}, i=1,2,3,4, the transfer functions are similar, because they are transfer functions between the tires and their wheel axle. Fig. 4(a) and 4(b) which are for the tractor are similar, and Fig. 4(c) and 4(d) which are for the trailer are similar too.

From Fig. 4(e), one can see that the amplitudes of H_{51} and H_{52} are close to each other, i.e., the vertical response of the tractor due to its two wheel set inputs is about the same. The amplitudes of H_{53} and H_{54} are much smaller than H_{51} and H_{52}. It can be realized that the tractor response is more influenced by the first and second wheel sets than by the third and fourth wheel axles.

As seen in Fig. 4(f), the amplitudes of H_{61} and H_{62} are larger than those of H_{63} and H_{64}, i.e., the driver seat response is dominantly influenced by the tractor wheel axles. As seen in Fig. 4(g), the amplitudes of H_{71} and H_{72} are larger than those of H_{73} and H_{74}, i.e., the pitch response of the tractor is majorly influenced by the tractor wheel axles. The pitch response of the tractor due to the first and second wheel axles can be about the same, because of the closeness of the amplitudes of H_{71} and H_{72}

As seen in Fig. 4(h), the amplitudes of H_{82} and H_{83} are larger than those of H_{81} and H_{84}, especially for frequencies below 1 Hz. As expected, the draw bar is mainly influenced by the second and third wheel axles.

From Fig. 4(i), the amplitudes of H_{93} and H_{94} are higher than those of H_{91} and H_{92}, i.e., the trailer response is dominated by the third and fourth wheel axles inputs.

From the observation of transfer functions, their characteristics can be summarized as follows:

1. The response of each unsprung mass is dominated by its own wheel axle input.
2. The driver seat response is dominated by the first and second wheel axle inputs.
3. The vertical and pitch response of the tractor are dominantly influenced by the first and second wheel axle inputs.
4. The draw bar response is dominated by the second and third wheel axle inputs.
5. The tractor response is dominated by the third and fourth wheel axle inputs.

B. Assessment of Ride Quality Parameters

1. The Ride Quality of the Driver

Fig. 5(a) shows the RMS accelerations of the driver seat in 1/3 octave band for different vehicle speeds (60, 75, 90 and 100 km/hr), when the road surface is assumed to be ISO road class B (good), and the laden condition is half-laden for the tractor and half-laden for the trailer. The ISO comfort criteria for 1-hour and 8-hour are also plotted. One can see that the ride quality of the driver can be in a quite good condition at different vehicle speeds. The variation of vehicle speed does not affect the driver's comfort very much.

The standard deviations of the acceleration of the driver seat calculated based on Eq. (74) for different vehicle speeds are also listed in Table 3(a). As expected, the higher the vehicle speed, the higher the standard deviation.

Fig. 5(b) shows the RMS accelerations of the driver seat in 1/3 octave band for different road surfaces (ISO road classes A, B, C and D), when the vehicle speed is assumed to be 90 km/hr, and the laden condition is half-laden for the tractor and half-laden for the trailer. The driver's ride quality is within the ISO 2631 8-hour comfort limit except for the ISO road class D (poor). For different classes of road conditions, the RMS accelerations varies largely as expected, because the road surfaces are defined by ISO 2631 [1] which characterizes the different classes of the road roughness in a large scale of order. The standard deviations of the driver seat are tabulated in Table 3(b). The better the road conditions, the lower the standard deviations.

Fig. 5(c) shows the RMS accelerations of the driver seat in 1/3 octave band for different laden conditions, such as Full/Full, Full/Empty, Empty/Full, Half/Half and Empty/Empty, when the vehicle speed is assumed to be 90 km/hr, and the ISO road class is B (good). The driver's ride quality is not much influenced by the laden conditions. However, as shown in Table 3(c) the standard deviation of driver seat acceleration is larger for the Empty/Empty laden condition. It is also interesting to note that the Full/Empty laden condition will provide better ride quality for the driver than the Empty/Full laden condition, and the Half/Half laden condition is just somewhere in between the Full/Empty and the Empty/Full laden conditions.

2. Suspension travel

Table 4(a) shows the standard deviations of suspension travels for the four wheel sets, corresponding to the cases shown in Fig. 5(a). For the comparison purpose, the standard deviations of suspension travel are also plotted in Fig. 6(a) One can see that the standard deviations of the suspension travel for the wheel axles of the trailer are higher than those for the tractor. As the increase of the vehicle speed, the standard deviation of the suspension travel can be expected to be higher.

Table 4(b) shows the standard deviations of suspension travels for the four wheel sets, corresponding to the cases shown in Fig. 5(b). The standard deviations of the suspension travel are also plotted in Fig. 6(b). As one can see, the better the road surface condition, the lower the standard deviations of the suspension travel. Again, the trailer will results in higher suspension travels than the tractor.

Table 4(c) shows the standard deviations of suspension travels for the four wheel sets, corresponding to the cases shown in Fig. 5(c). The standard deviations of the suspension travel are also plotted in Fig. 6(c). As expected, the higher the laden, the higher the standard deviations of the suspension travels. In particular, the standard deviations of the suspension travels for the case of Half/Half condition is just somewhere in between the Full/Full and Empty/Empty laden conditions.

3. Road holding

Figs. 7(a)-7(c) show the standard deviations of the road holdings corresponding to the cases in Figs. 5(a)-5(c). The values of the standard deviations of the road holdings are listed in Table 5(a)-5(c). As shown in Fig. 7(a), the trailer's tires have smaller standard deviations of the road holding than the tractor's, i.e., the trailer have better road holding ability than the tractor. As the increase of the vehicle speed, the chance of the departure of the tire from the road is increased.

From Fig. 7(b), the worse the road condition, the worse the road holding. From Fig. 7(c), one can see that the standard deviations of the road holdings are not much different for different laden conditions; however, the trailer have much better road holding ability than the tractor.

4. Dynamic tire load

The dynamic tire load are directly related to the road holding as shown in Eqns. (57)-(60). Figs. 8(a)-8(c) and Table 6(a)-6(c) are corresponding to the cases in Figs. 7(a)-7(c) and Table 5(a)-5(c) respectively. From the observation of Fig. 8(a)-8(c), the higher the vehicle speed, the higher the contact force; the worse the road condition, the higher the contact force; and the laden conditions make no many differences in contact forces. In general, the tractor's tires sets are subjected to higher contact forces than the trailer's. The tire wear in the tractor can be expected higher than that in the trailer.

5. The tractor and trailer body acceleration

The standard deviations of the accelerations of $\ddot{z}_1$-$\ddot{z}_{12}$ which are defined as shown in Fig. 2. Figs. 9(a)-9(c) for different vehicle speeds, different road conditions and different pay-loads are presented respectively. In general, the standard deviations of the accelerations at the center of gravity of the tractor and trailer are smaller than elsewhere. Both the standard deviations of the tractor and trailer body acceleration are almost the same near the locations of the center of gravity. The effects of vehicle speed and road condition are significant, while the loden conditions have little influence. For better ride quality of the cargo, the cargo should be placed on the trailer in the preference to on the tractor. The cargo should not be placed as near as the center of gravity of the tractor or trailer for better ride quality of the cargo. As expected, the higher the vehicle speed, and the worse the road condition, the worse the ride quality of the cargo.

VIII. Conclusions

This paper shows the ride quality analysis of the full tractor and trailer. Firstly, the 9 DOF riding model is developed. The tractor and trailer are assumed to be rigid bodies subjecting to the vertical and pitch motion only. The suspension system and tires are modeled to be linear spring-damper elements. The model is also assumed to be symmetric along the moving direction. The displacement input of stationary ergodic Gaussian random road surface defined by ISO is adopted in the paper. The frequency response functions (transfer functions) can be defined between the input and output vectors of the linear system. Therefore, the output power spectral density (PSD) function of the system related to the PSD function of the road input can be determined through the frequency domain analysis. As the output PSD function for the accelerations of the vehicle have been obtained, the root-mean square values of acceleration as a function of frequency in 1/3 octave band can be obtained. Finally, the riding quality of the driver seat can be evaluated in comparison to the ISO 2631 vertical acceleration spectra[1]. The system parameters, including suspension travel, road holding and dynamic tire load between the tire and the road are also studied. They are important factors for the design of the tractor and trailer system. The results can be used for further analysis, such as the cargo ride analysis and road damage evaluation. The developed model can also be utilized for the optimum design of system parameters.

Acknowledgment

The authors gratefully acknowledge the support of the work by National Science Council, Republic of China, under grant NSC84-2212-E-020-009

Reference

1. ISO, 1978, "Guide for the Evaluation of Human Exposure to Whole-Body Vibration", 2nd ed., International Standard 2631-1978(E), *International Organization for Standardization.*
2. Lee, R. and F., Pradko, 1968, "Analytical Analysis of Human Vibration", *SAE Transaction*, Paper No. 680091, pp. 346-370.
3. Stikeleather, L.F., 1976, "Review of Ride Vibration Standards and Tolerance Criteria", *SAE Transaction*, Paper No. 760413, pp.1460-1467
4. Ravalard, Y., and D., Coutellier and S.Masfrand, 1994, "Dynamical Behavior of Articulated Train Car and Influence on Vertical Comfort", *Transaction of CSME*, Vol. 18, No. 3, pp.269-283.
5. Sperling, B., 1956, "Beitag zur Beuteilung des Fahrkomforts in Schienenfahrzeugen," *Glasers* Ann.80 .pp314 a 318.
6. Ryba, D., 1974, "Improvement in Dynamic Characteristics of Automobile Suspension Systems, Part 1. Two Mass

System," *Vehicle System Dynamics*, Vol. 3, pp.17-46.
7. Dahlberg, T., 1979, "An Optimized Speed-Controlled Suspension of a 2-DOF Vehicle Traveling On a Randomly Profiled Road," *Journal of Sound and Vibration*, Vol. 62, pp.541-546.
8. A. Hac, 1985, "Suspension Optimization of a 2-DOF Vehicle Model Using a Stochastic Optimal Control technique," *Journal of Sound and Vibration*, Vol. 100, pp.343-357.
9. Demic, M., 1992, "Optimization of Characteristics of Elasto-damper Elements of Cars from the aspect of comfort and handling," *International of Vehicle Design*, Vol. 13, No. 1, pp. 29-46.
10. Elmadany, M.M., 1987, "A Procedure for Optimization of Truck Suspension," *Vehicle System Design*, Vol. 16, pp.297-312.
11. Vaduri, S., and E. H., Law, 1993, "Development of a Simulation for Assessment of Ride Quality of Tractor and Trailer," *SAE* paper 932940.
12. Margolis, D. and D., Edeal, 1989, "Modeling and Control of Large Flexible Frame Vehicles Using Bond Graphics," *SAE* paper 892488.
13. ElMadany, M.M., and Z., Abduljabbar, 1990, "Design Evaluation of Advanced Suspension Systems for Truck Ride comfort," *Computers & Structures*, Vol. 36, No.2, pp. 321-331.
14. Clark, S. K.(ed), August 1981, "Mechanics of Pneumatic Tires," *US Department of Transportation*, NHTSA, DOT HS 805952.
15. Iwan, W.D., and Yang, I.M. , 1972, "Application of Statistical Linearization techniques to Nonlinear Muti-Degree of Freedom Systems.," *Journal of applied Mechanics*, Vol. 39, pp.545-550.
16. Atalik, T.S., and S., Utku, 1976, "Stochastic Linearization of Muti-degree of-freedom Non-linear systems," *Earthquake Engineering and Structural Dynamics*, Vol. 4, pp.411-420.
17. ElMadany, M. M., and M.A., Dokainish, 1980, "Articulated Vehicle Dynamic Analysis Using Equivalent Linearization Technique," *SAE Transactions*, Vol. 89, Paper 801421, pp.4506-4517.
18. Dohi, M., and Y., Maruyama, 1990, "Ride Comfort Optimization for Commercial Trucks," *SAE Transaction*, Vol. 99, No. 2, pp.890-902.
19. Sun, J., 1987, "Frequency Spectral Analysis of Bridge-Vehicle System due to Road Surface Roughness," *Vehicle System Dynamics*, Vol. 16, pp.227-239.
20. Del Castillo, J.M., P., Pintado, and F.G., Benitez, 1990, "Optimization for Vehicle Suspension II: Frequency Domain," *Vehicle System Dynamics*, Vol. 19, p.p.331-352.
21. Pintado, P., and F.G., Benitez, 1990, "Optimization for Vehicle Suspension II: Time Domain," *Vehicle System Dynamics*, Vol. 19, pp.273-288.
22. ISO, 1982, "Reporting Vehicle Road Surface Irregularities," ISO/TC108/SC2/WG4 N57.
23. Bendat, J. S., 1986, *Random Data Analysis and Measurement Procedures*, 2nd ed., John Wiley & Sons, Inc..

Appendix A: Definition of System Matrices

$$[M]=\begin{bmatrix} m_1 & 0 & 0 & 0 & 0 & 0 & 0 & 0 & 0 \\ 0 & m_2 & 0 & 0 & 0 & 0 & 0 & 0 & 0 \\ 0 & 0 & m_3 & 0 & 0 & 0 & 0 & 0 & 0 \\ 0 & 0 & 0 & m_4 & 0 & 0 & 0 & 0 & 0 \\ 0 & 0 & 0 & 0 & m_5+\frac{m_6 l_6}{l_5+l_6} & 0 & \frac{m_6 l_6 l_7}{l_5+l_6} & \frac{m_6 l_5 l_6 - I_6}{l_5+l_6} & 0 \\ 0 & 0 & 0 & 0 & m_7+\frac{m_6 l_5}{l_5+l_6} & 0 & m_7 l_7+\frac{m_6 l_5 l_7}{l_5+l_6} & m_7(l_5+l_6)+\frac{m_6 l_5^2+I_6}{l_5+l_6} & m_7 l_8 \\ 0 & 0 & 0 & 0 & 0 & m_8 & 0 & 0 & 0 \\ 0 & 0 & 0 & 0 & \frac{m_6 l_6 l_7}{l_5+l_6} & 0 & I_5+\frac{m_6 l_6 l_7^2}{l_5+l_6} & \frac{m_6 l_5 l_6 l_7 - I_6 l_7}{l_5+l_6} & 0 \\ 0 & 0 & 0 & 0 & -\frac{m_6 l_5 l_8}{l_5+l_6} & 0 & -\frac{m_6 l_5 l_7 l_8}{l_5+l_6} & -\frac{I_6 l_8 + m_6 l_5^2 l_8}{l_5+l_6} & I_7 \end{bmatrix}$$

(A-1)

$$[C]=\begin{bmatrix} c_{s1}+c_{t1} & 0 & 0 & 0 & -c_{s1} & 0 & c_{s1}l_1 & 0 & 0 \\ 0 & c_{s2}+c_{t2} & 0 & 0 & -c_{s2} & 0 & -c_{s2}l_2 & 0 & 0 \\ 0 & 0 & c_{s3}+c_{t3} & 0 & -c_{s3} & 0 & -c_{s3}l_7 & -c_{s3}(l_5+l_6) & -c_{s3}(l_8-l_3) \\ 0 & 0 & 0 & c_{s4}+c_{t4} & -c_{s4} & 0 & -c_{s4}l_7 & -c_{s4}(l_5+l_6) & -c_{s4}(l_8+l_4) \\ -c_{s1} & -c_{s2} & 0 & 0 & c_8+c_{s1}+c_{s2} & -c_8 & -c_8l_9-c_{s1}l_1+c_{s2}l_2 & 0 & 0 \\ 0 & 0 & -c_{s3} & -c_{s4} & c_{s3}+c_{s4} & 0 & c_{s3}l_7+c_{s4}l_7 & (c_{s3}+c_{s4})(l_5+l_6) & c_{s3}(l_8-l_3)+c_{s4}(l_8+l_4) \\ 0 & 0 & 0 & 0 & -c_8 & c_8 & c_8l_9 & 0 & 0 \\ c_{s1}l_1 & -c_{s2}l_2 & 0 & 0 & -c_8l_9-c_{s1}l_1+c_{s2}l_2 & c_8l_9 & c_8l_9^2+c_{s1}l_1^2+c_{s2}l_2^2 & 0 & 0 \\ 0 & 0 & c_{s3}l_3 & -c_{s4}l_4 & -c_{s3}l_3+c_{s4} & 0 & -c_{s3}l_7l_3+c_{s4}l_7l_4 & -c_{s3}(l_5+l_6)l_3+c_{s4}(l_5+l_6)l_4 & -c_{s3}(l_8-l_3)l_3+c_{s4}(l_8+l_4)l_4 \end{bmatrix}$$

(A-2)

$$[K]=\begin{bmatrix} k_{s1}+k_{t1} & 0 & 0 & 0 & -k_{s1} & 0 & k_{s1}l_1 & 0 & 0 \\ 0 & k_{s2}+k_{t2} & 0 & 0 & -k_{s2} & 0 & -k_{s2}l_2 & 0 & 0 \\ 0 & 0 & k_{s3}+k_{t3} & 0 & -k_{s3} & 0 & -k_{s3}l_7 & -k_{s3}(l_5+l_6) & -k_{s3}(l_8-l_3) \\ 0 & 0 & 0 & k_{s4}+k_{t4} & -k_{s4} & 0 & -k_{s4}l_7 & -k_{s4}(l_5+l_6) & -k_{s4}(l_8+l_4) \\ -k_{s1} & -k_{s2} & 0 & 0 & k_8+k_{s1}+k_{s2} & -k_8 & -k_8l_9-k_{s1}l_1+k_{s2}l_2 & 0 & 0 \\ 0 & 0 & -k_{s3} & -k_{s4} & k_{s3}+k_{s4} & 0 & k_{s3}l_7+k_{s4}l_7 & (k_{s3}+k_{s4})(l_5+l_6) & k_{s3}(l_8-l_3)+k_{s4}(l_8+l_4) \\ 0 & 0 & 0 & 0 & -k_8 & k_8 & k_8l_9 & 0 & 0 \\ k_{s1}l_1 & -k_{s2}l_2 & 0 & 0 & -k_8l_9-k_{s1}l_1+k_{s2}l_2 & c_8l_9 & k_8l_9^2+k_{s1}l_1^2+k_{s2}l_2^2 & 0 & 0 \\ 0 & 0 & k_{s3}l_3 & -k_{s4}l_4 & -k_{s3}l_3+k_{s4} & 0 & -k_{s3}l_7l_3+k_{s4}l_7l_4 & -k_{s3}(l_5+l_6)l_3+k_{s4}(l_5+l_6)l_4 & -k_{s3}(l_8-l_3)l_3+k_{s4}(l_8+l_4)l_4 \end{bmatrix}$$

(A-3)

$$[k'] = \begin{bmatrix} k_{t_1} & 0 & 0 & 0 \\ 0 & k_{t_2} & 0 & 0 \\ 0 & 0 & k_{t_3} & 0 \\ 0 & 0 & 0 & k_{t_4} \end{bmatrix} \quad \text{(A-4)}$$

$$[c'] = \begin{bmatrix} c_{t_1} & 0 & 0 & 0 \\ 0 & c_{t_2} & 0 & 0 \\ 0 & 0 & c_{t_3} & 0 \\ 0 & 0 & 0 & c_{t_4} \end{bmatrix} \quad \text{(A-5)}$$

Apppendix B: Symbol Description

Symbol	Description
$z_1=y_1$	Vertical displacement of unsprung mass m_1
$z_2=y_2$	Vertical displacement of unsprung mass m_2
$z_3=y_3$	Vertical displacement of unsprung mass m_3
$z_4=y_4$	Vertical displacement of unsprung mass m_4
$z_5=y_5$	Vertical displacement of the tractor
$z_8=y_6$	Vertical displacement of the driver seat
$\theta_1=y_7$	Pitch angle of the tractor
$\theta_2=y_8$	Pitch angle of the draw bar
$\theta_3=y_9$	Pitch angle of the trailer
x_1	Displacement road input of the front wheel set of the tractor
x_2	Displacement road input of the rear wheel set of the tractor
x_3	Displacement road input of the front wheel set of the trailer
x_4	Displacement road input of the rear wheel set of the trailer
m_1	Mass of the first wheel axle
m_2	Mass of the second wheel axle
m_3	Mass of the third wheel axle
m_4	Mass of the forth wheel axle
m_5	Mass of the empty tractor
m_6	Mass of the draw bar
m_7	Mass of the empty trailer
m_8	Mass of the driver seat
I_5	Moment of inertia of the empty tractor
I_6	Moment of inertia of the draw bar
I_7	Moment of inertia of the empty trailer
w_1	Loading capacity of the tractor
w_2	Loading capacity of the trailer
R_{w_1}	Ratio of loading capacity of the tractor
R_{w_2}	Ratio of loading capacity of the trailer
k_{t_1}	Spring constant of the front tire of the tractor
k_{t_2}	Spring constant of the rear tire of the tractor
k_{t_3}	Spring constant of the front tire of the trailer
k_{t_4}	Spring constant of the rear tire of the trailer
k_{s_1}	Spring constant of the front suspension of the tractor
k_{s_2}	Spring constant of the rear suspension of the tractor
k_{s_3}	Spring constant of the front suspension of the trailer
k_{s_4}	Spring constant of the rear suspension of the trailer
k_d	Spring constant of the driver seat
l_1	The length between the front tire and the center gravity of tractor
l_2	The length between the rear tire and the center gravity of tractor
l_3	The length between the front tire and the center gravity of trailer
l_4	The length between the rear tire and the center gravity of trailer
l_5	The length between the tractor end and the center gravity of raw bar
l_6	The length between the trailer head and the center gravity of draw bar
l_7	The length between the tractor center gravity and the tractor end
l_8	The length between the trailer center gravity and the draw bar end
l_9	The length between the seat and the center gravity of the tractor
l_{10}	The length between the head of the tractor and the driver seat
l_{11}	The length between the center gravity of trailer and the trailer end

Appendix C: Parameter Values and Units of the Full Tractor and Trailer

Symbol	Value	Units
m_1	800	kg
m_2	800	kg
m_3	800	kg
m_4	800	kg
m_5	4000	kg
m_6	200	kg
m_7	3600	kg
m_8	100	kg
I_5	8500	$kg-m^2$

I_6	45	$kg-m^2$
I_7	7500	$kg-m^2$
w_1	12400	kg
w_2	12400	kg
k_{t_1}	800000	N/m
k_{t_2}	800000	N/m
k_{t_3}	800000	N/m
k_{t_4}	800000	N/m
k_{s_1}	80000	N/m
k_{s_2}	80000	N/m
k_{s_3}	80000	N/m
k_{s_4}	80000	N/m
k_d	4000	N/m
c_{t_1}	2000	$N-s/m$
c_{t_2}	2000	$N-s/m$
c_{t_3}	2000	$N-s/m$
c_{t_4}	2000	$N-s/m$
c_{s_1}	30000	$N-s/m$
c_{s_2}	30000	$N-s/m$
c_{s_3}	30000	$N-s/m$
c_{s_4}	30000	$N-s/m$
c_d	250	$N-s/m$
l_1	1.6	m
l_2	1.4	m
l_3	1.7	m
l_4	1.3	m
l_5	0.85	m
l_6	0.8	m
l_7	2.7	m
l_8	2.4	m
l_9	1.3	m
l_{10}	1.0	m
l_{11}	2.6	m
Full/Full condition	R_{w_1}=1, R_{w_2}=1	l_{w_1}=0, l_{w_2}=0
Half/Half condition	R_{w_1}=0.5, R_{w_2}=0.5	l_{w_1}=0, l_{w_2}=0
Empty/Empty condition	R_{w_1}=0, R_{w_2}=0	l_{w_1}=0, l_{w_2}=0

Table 1. Road Roughness Proposed by ISO [22]

Degree of roughness $S_g(\Omega_0)$, $10^{-6}m^2/cycles/m$		
Road Class	Range	Geometric Mean
A (Very Good)	<8	4
B (Good)	8-32	16
C (Average)	32-128	64
D (Poor)	128-512	256
E(Very Poor)	512-2048	1024
F	2048-8192	4096
G	8192-32768	16384
H	>32768	

Table 2. Natural frequencies of the system

Mode	Natural Frequency (Hz)
1	0.46936
2	0.47427
3	0.91371
4	1.03105
5	1.06685
6	5.28072
7	5.28069
8	5.28766
9	5.28916

Table 3. Standard deviation of driver seat acceleration

(a) Vehicle speed (ISO road class: B, Laden condition half/half)

Speed (km/hr)	$\sigma_{\ddot{y}_s}$ $(m/\sec^2)$
60	.3668
75	.4762
90	.5449
100	.5717

(b) Road (Vehicle speed 90 km/hr, Laden condition half/half)

ISO road class	$\sigma_{\ddot{y}_s}$ $(m/\sec^2)$
A(Very Good)	.2724
B(Good)	.5449
C(Average)	1.089
D(Poor)	2.179

(c) Laden (ISO road class: B, Vehicle speed 90 km/hr)

Laden (Tractor/Trailer)	$\sigma_{\ddot{y}_s}$ $(m/\sec^2)$
Full/Full	.5131
Full/Empty	.5146
Empty/Full	.5678
Half/Half	.5449
Empty/Empty	.5687

Table 4. Standard deviation of suspension travel

(a) Vehicle speed (ISO road class: B, Laden condition half/half)

Speed (km/hr)	σ_{d_1} (m)	σ_{d_2} (m)	σ_{d_3} (m)	σ_{d_4} (m)
60	.003310	.003886	.005363	.005919
75	.003725	.004185	.005921	.006556
90	.004130	0.04511	.006400	.007161
100	.004377	0.004732	.006690	.007545

(b) Road (Vehicle speed 90 km/hr, Laden condition half/half)

ISO Road Class	σ_{d_1} (m)	σ_{d_2} (m)	σ_{d_3} (m)	σ_{d_4} (m)
A(Very Good)	.002065	.002255	.003200	.003580
B(Good)	.004130	.004511	.006400	.007160
C(Average)	.008261	.009023	.001280	.014321
D(Poor)	.016523	.018047	.025600	.028643

(c) Laden (ISO road class: B, Vehicle speed 90 km/hr)

Laden (Tractor/Trailer)	σ_{d_1} (m)	σ_{d_2} (m)	σ_{d_3} (m)	σ_{d_4} (m)
Full/Full	.005119	.005637	.007048	.008187
Full/Empty	.005132	.005618	.005650	.006248
Empty/Full	.002811	.003105	.006755	.008251
Half/Half	.004131	.004512	.006400	.007161
Empty/Empty	.002817	.003088	.005487	.006203

Table 5. Standard deviation of road holding

(a) Vehicle speed (ISO road class: B, Laden half/half)

Speed(km/hr)	σ_{h_1} (m)	σ_{h_2} (m)	σ_{h_3} (m)	σ_{h_4} (m)
60	.003596	.003863	.002999	.002754
75	.005485	.004960	.003319	.002940
90	.006676	.005625	.003547	.003106
100	.007148	.005860	.003669	.003211

(b) Road (Vehicle speed 90 km/hr, Laden half/half)

ISO Road Class	σ_{h_1} (m)	σ_{h_2} (m)	σ_{h_3} (m)	σ_{h_4} (m)
A(Very Good)	.003338	.002813	.001773	.001553
B(Good)	.006676	.005625	.003547	.003106
C(Average)	.01335	.01125	.007093	.006212
D(Poor)	.02670	.02250	.01419	.01242

(c) Laden (ISO road class: B, Vehicle speed 90 km/hr)

Laden (Tractor/Trailer)	σ_{h_1} (m)	σ_{h_2} (m)	σ_{h_3} (m)	σ_{h_4} (m)
Full/Full	.006659	.005658	.003581	.003094
Full/Empty	.006666	.005663	.003310	.003329
Empty/Full	.006739	.005521	.003569	.003114
Half/Half	.006676	.005625	.003547	.003106
Empty/Empty	.006744	.005526	.003321	.003327

Table 6. Standard deviation of tire/road contact force

(a) Vehicle speed (ISO road class: B, Laden condition half/half)

Speed(km/hr)	σ_{f_1} (N)	σ_{f_2} (N)	σ_{f_3} (N)	σ_{f_4} (N)
60	15.7764	15.9214	15.3587	15.2907
75	17.7551	17.4025	16.2929	16.1708
90	19.3389	18.5529	17.0826	16.9394
100	20.1163	19.1313	17.5496	17.3980

(b) Road (Vehicle speed 90 km/hr , Laden half/half)

ISO Road Class	σ_{f_1} (N)	σ_{f_2} (N)	σ_{f_3} (N)	σ_{f_4} (N)
A(Very Good)	9.66947	9.27645	8.5413	8.46973
B(Good)	19.3389	18.5529	17.0826	16.9439
C(Average)	38.6778	37.1058	34.1765	33.8789
D(Poor)	77.3557	74.2116	68.3305	67.7578

(c) Laden (ISO road class: B, Vehicle speed condition 90 km/hr)

Laden (Tractor/Trailer)	σ_{f_1} (N)	σ_{f_2} (N)	σ_{f_3} (N)	σ_{f_4} (N)
Full/Full	19.3202	18.5690	17.0882	16.9316
Full/Empty	19.3263	18.5744	17.0321	17.0112
Empty/Full	19.4068	18.4964	17.0873	16.9352
Half/Half	19.3389	18.5529	17.0826	16.9394
Empty/Empty	19.4122	18.4957	17.0348	17.0110

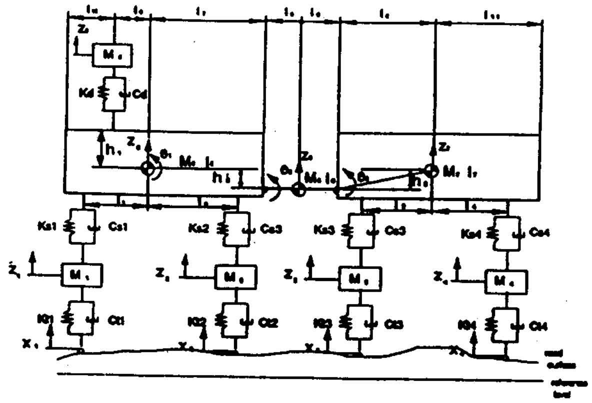

Fig. 1. 9 DOF full tractor/trailer riding model

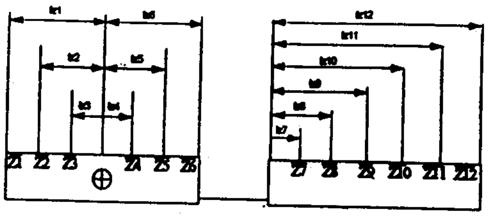

Fig. 2. Definition of $\bar{Z}_1 \sim \bar{Z}_{12}$

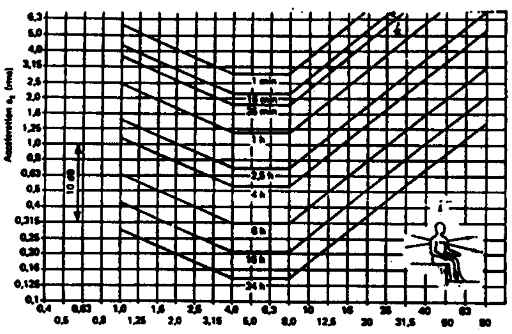

Fig. 3. Limits of whole-body vibration for fatigue in vertical direction [1]

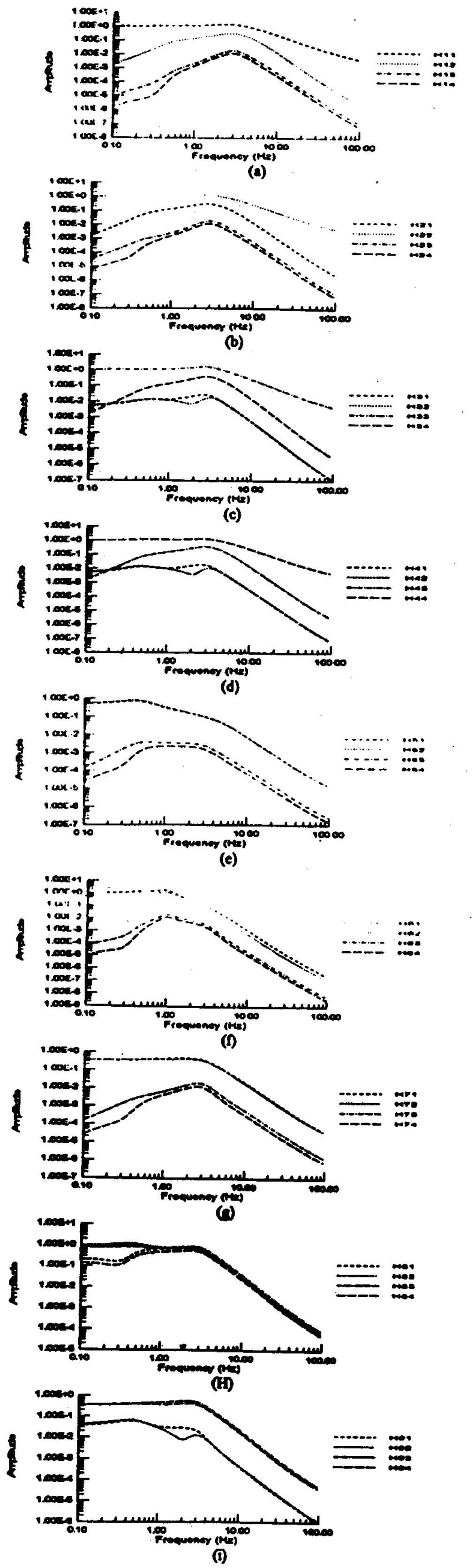

Fig. 4. Transfer functions for the 9 DOF full tractor and trailer model

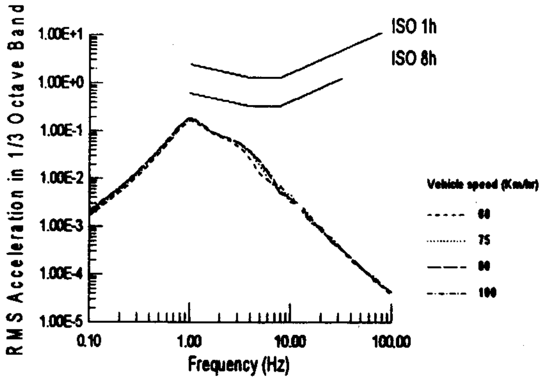

(a) Vehicle speed (ISO road class B, Laden condition half / half)

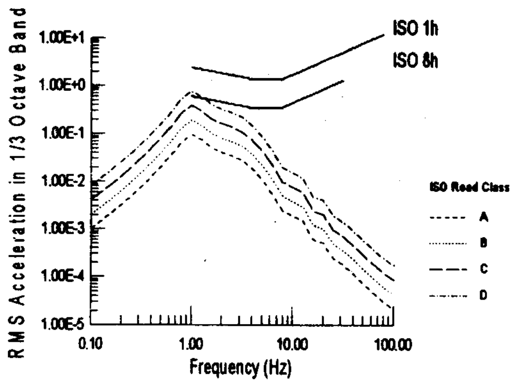

(b)ISO road class (Vehicle speed 90 km/hr, Laden condition half/half)

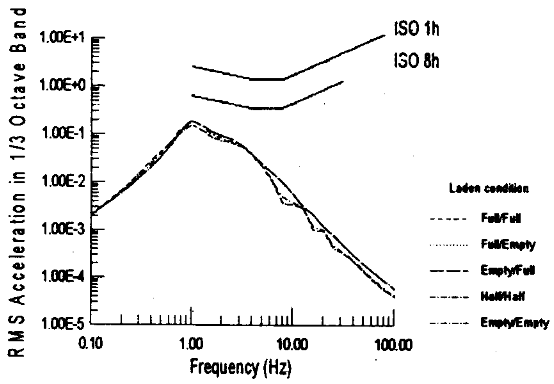

(c) Laden condition (ISO road class: B, Vehicle speed 90 km/hr)

Fig. 5. RMS Acceleration of driver-seat in 1/3 Octave Band

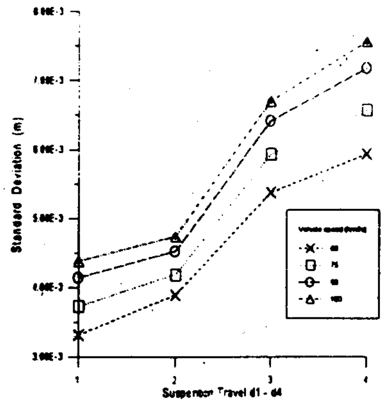

(a) Vehicle speed (ISO road class B ,Laden condition half/half)

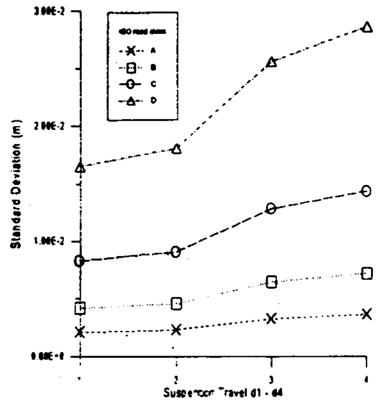

(b) ISO road class (Vehicle speed 90 km/hr, Laden condition half/half)

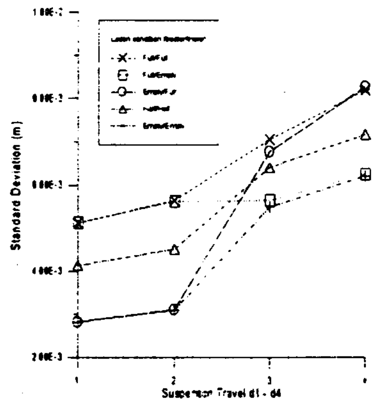

(c) Laden(ISO road class B, Vehicle speed 90 km/hr)

Fig. 6. Standard deviation of suspension travel

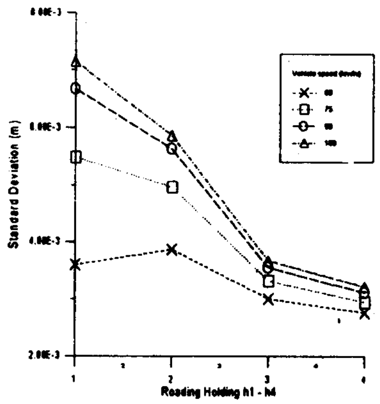

(a) Vehicle speed (ISO road class B, Laden condition half/half)

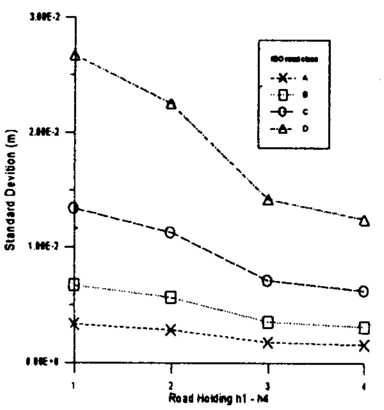

(b) ISO road class (Vehicle speed 90 km/hr, Laden condition half/half)

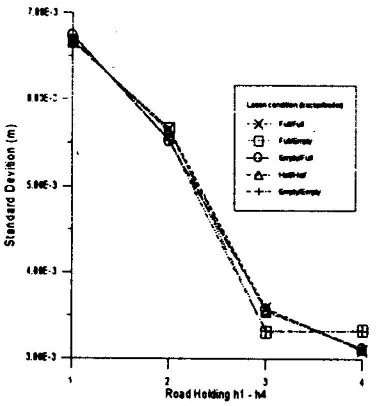

(c) Laden condition (ISO road class B, Vehicle speed 90 km/hr)

Fig. 7. Standard deviation of road holding

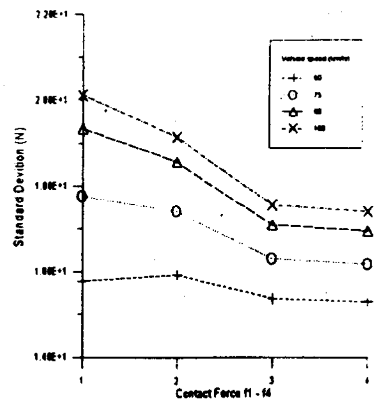

(a) Vehicle speed (ISO road class B, Laden condition half/half)

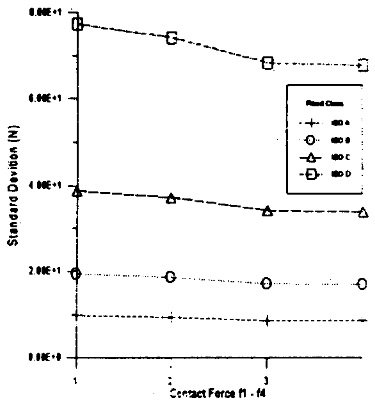

(b) ISO road class(Vehicle speed 90 km/hr, Laden condition half/half)

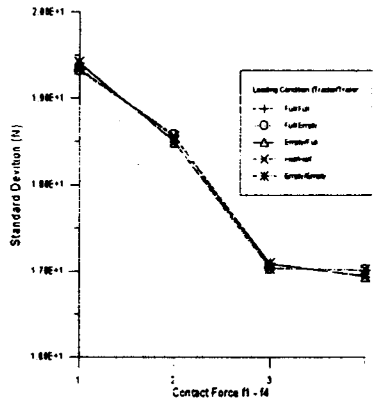

(c) Laden condition (ISO road class B, Vehicle speed 90 km/hr)

Fig. 8. Standard deviation of contact forces between tire/road

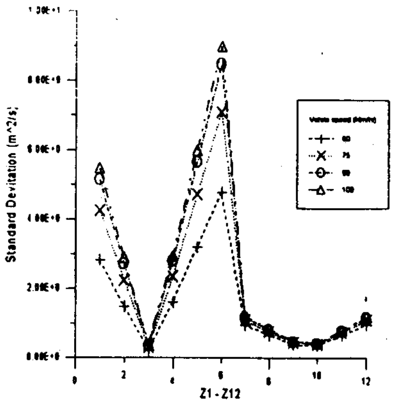

(a) Vehicle speed (ISO road class B, Laden condition half/half)

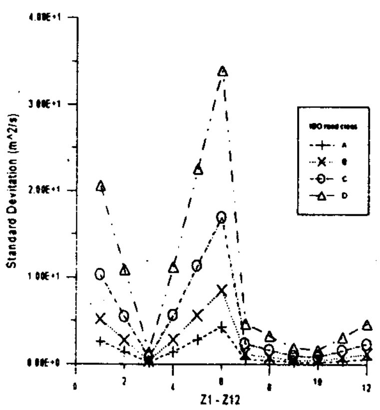

(b) ISO road class(Vehicle speed 90 km/hr, Laden condition half/half)

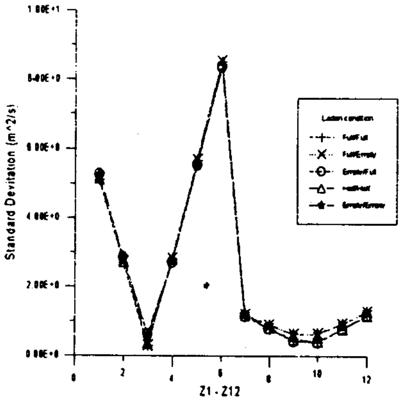

(c) Laden condition (ISO road class B, Vehicle speed 90 km/hr)

Fig. 9. Standard deviation of tractor/trailer acceleration